East Asian Journal on Applied Mathematics
doi: 10.4208/eajam.181016.300517d

Vol. 7, No. 4, pp. 837-851
November 2017

Pinning Effect on Current-Induced Domain Wall Motion in Nanostrip

Lei Yang*

Faculty of Information and Technology, Macau University of Science and Technology, Macao SAR.

Received 18 October 2016; Accepted (in revised version) 30 May 2017.

Abstract. Pinning effect on current-induced magnetic transverse domain wall dynamics in nanostrip is studied for its potential application to new magnetic memory devices. In this study, we carry out a series of calculations by solving generalized Landau-Lifshitz equation involving a current spin transfer torque in one and two dimensional models. The critical current for the transverse wall depinning in nanostrip depends on the size of artificial rectangular defects on the edges of nanostrip. We show that there is intrinsic pinning potential for a defect such that the transverse wall oscillates damply around the pinning site with an intrinsic frequency if the applied current is below critical value. The amplification of the transverse wall oscillation for both displacement and maximum value of m_3 is significant by applying AC current and current pulses with appropriate frequency. We show that for given pinning potential, the oscillation amplitude as a function of the frequency of the AC current behaves like a Gaussian distribution in our numerical study, which is helpful to reduce strength of current to drive the transverse wall motion.

AMS subject classifications: 35R05, 58J35, 35Q60.

Key words: Spin current, domain wall motion, Landau-Lifshitz equation.

1. Introduction

Recent research activities in precise control and manipulation of magnetic domain structures have been focused on magnetization dynamics driven by current due to its possible application on the new digital data storage [13, 14]. From the application point of view, the current induced magnetization reversal opens a way to control and manipulate the magnetization dynamics, and it is much better to control the spatial region and individual magnetic elements compared with the conventional magnetic field induced reversal. For technological applications, the domain walls must be moved on much shorter timescales which is easier to be achieved by a current. High current densities used for the experiments yield the local higher temperature, which induces many magnons. Therefore, high velocity

*Corresponding author. *Email address:* leiyang@must.edu.mo (L. Yang)

 ©2017 Global-Science Press

https://doi.org/10.4208/eajam.181016.300517d Published online by Cambridge University Press

of domain wall motion and low current density are important issues to optimize magnetic device performance. To realize lower current density, further understanding of the driving mechanism as well as extrinsic effects, such as pinning, are necessary.

Magnetic domain wall dynamics induced by current in magnetic nanostrip has received great interest both experimentally and numerically [2,4,5,8,10,12,15,21,22,27] for applications in magnetoelctronic devices. In the perfect magnetic nanostrip without defects, the domain wall can move along the strip when an external magnetic field or polarized current is applied along the wire axis. In realistic nanostrips, domain walls are not completely free to move. There are various pinning sources such as kinds of defects and roughness. Pinning effect of defects on domain wall motion is important and interesting phenomena and has attracted much attention in recent years [6, 7, 24]. The control of domain wall is very important in the study of current induced domain wall motion. One of the most feasible domain wall control methods is to place defects on the magnetic nanowire [11, 19]. The dynamics of magnetization under the applied spin current is modeled by the generalized Landau-Lifshitz equation with a spin transfer torque term [26]. Numerical methods have been investigated to solve the generalized Landau-Lifshitz system [20, 23].

In this paper, we study the pinning effect on the transverse domain wall motion induced by current spin torque in one and two dimensional models numerically. In Section 3, we construct the nanostrip with rectangular defects of various size on the edges and initial steady transverse domain wall. The two dimensional numerical calculation is carried out for the full generalized Landau-Lifshitz equation with current spin transfer torque, and we provide insight on the pinning effect of the domain wall dynamics induced by current in the numerical results. In Section 4, a pinning potential term is involved to model defect in one dimensional system for more study on intrinsic pinning effect on the transverse wall motion by applying different kinds of current. We show the domain wall dynamics induced by DC current flows, nanosecond-long current pulses and AC current flows with different periods. By using current pulses and AC current, whose frequency is tuned to the precession one, the domain wall's oscillations can be amplified, which makes it possible to reduce the strength of current to drive the domain wall motion.

2. Model and Numerical Method

We consider domain wall propagation induced by current in a sufficiently long nanostrip. By assuming the current flow in the x direction along the long length of nanostrip, the spin transfer torque Γ_{st} [10, 27] is written as:

$$\Gamma_{st} = -\frac{b_J}{M_s^2}\mathbf{M}\times\left(\mathbf{M}\times\frac{\partial\mathbf{M}}{\partial x}\right) - \frac{c_J}{M_s}\mathbf{M}\times\frac{\partial\mathbf{M}}{\partial x}, \tag{2.1}$$

where $b_J = Pj_e\mu_B/eM_s$ and $c_J = \xi b_J$, P is the spin polarization of the current, j_e is the current density in the x direction, μ_B is Bohr magneton, and ξ is a dimensionless constant which describes the degree of the nonadiabaticity between the spin of the nonequilibrium conduction electrons and local magnetization.

https://doi.org/10.4208/eajam.181016.300517d Published online by Cambridge University Press

The generalized dynamic equation of the magnetization is described by Landau-Lifshitz-Gilbert equation in addition to the spin transfer torque as:

$$\frac{\partial \mathbf{M}}{\partial t} = -\gamma \mathbf{M} \times \mathbf{H}_{eff} + \frac{\alpha}{M_s}\mathbf{M} \times \frac{\partial \mathbf{M}}{\partial t} + \Gamma_{st}, \tag{2.2}$$

where $\mathbf{M}$ is the magnetization vector, M_s is the saturation magnetization, γ is the gyromagnetic ratio, α is the damping parameter, $\mathbf{H}_{eff}$ is the effective field written as:

$$\mathbf{H}_{eff} = \frac{A}{M_s^2}\Delta \mathbf{M} + \frac{H_k M_1}{M_s} e_x + \mu_0 \mathbf{H}_e - 4\pi M_3 e_z. \tag{2.3}$$

In (2.3), A is the exchange constant, $\frac{A}{M_s^2}\Delta \mathbf{M}$ is the exchange field, H_k is the anisotropy constant, μ_0 is the permeability of vacuum ($\mu_0 = 4\pi \times 10^{-7} N/A^2$ in the S.I.), $\mu_0 \mathbf{H}_e$ is the external applied magnetic field, and $4\pi M_3$ is the demagnetization field by considering the simple construction of transverse wall in thin nanotrip.

Substitute Γ_{st} into Eq. (2.2), then the generalized Landau-Lifshitz equation which is equivalent to the Landau-Lifshitz-Gilbert equation mathematically can be written as:

$$\frac{\partial \mathbf{M}}{\partial t} = -\gamma \mathbf{M} \times \mathscr{H}_{eff} + \frac{\alpha}{M_s}\mathbf{M} \times (\mathbf{M} \times \mathscr{H}_{eff}), \tag{2.4}$$

where the generalized effective field including the spin transfer torque is

$$\mathscr{H}_{eff} = \mathbf{H}_{eff} + \frac{b_J}{M_s^2}\mathbf{M} \times \frac{\partial \mathbf{M}}{\partial x} + \frac{c_J}{M_s}\frac{\partial \mathbf{M}}{\partial x}. \tag{2.5}$$

In this paper, pinning effect on transverse wall motion driven by current in thin nanostrip is investigated by two and one dimensional numerical calculations. Explicit fourth-order Runge-Kutta and second-order finite difference scheme are used to discretize (2.4) temporally and spatially with Newman boundary condition. The grid size is $2nm$ and $2nm \times 2nm$ in one and two dimensional calculation respectively. A sufficiently small time step $dt = 0.1M_s(1+\alpha^2)/\gamma A$ is necessary for the consideration of the stability of the numerical scheme due to the exchange term included in the effective field.

3. Current Driven Domain Wall Depinning

We consider long nanostrips with rectangular defects of various thickness and width on the edge of nanostrips. The defected strip is constructed by removing a rectangular defect from one edge of a perfect magnetic nano strip. The nano strip and the location of the defect are shown in Fig. 1 (a). The depth (height) and width of the rectangular defect are defined as d_D and w_D respectively. The strip is 400 nm long in the x direction and 50 nm wide in the y direction with defect in various size. Two dimensional magnetic calculations are carried out using the fourth-order Runge-Kutta method with Newman boundary conditions. The grid size is taken as 2×2 nm^2. The x axis is taken as the easy axis as well as the

https://doi.org/10.4208/eajam.181016.300517d Published online by Cambridge University Press

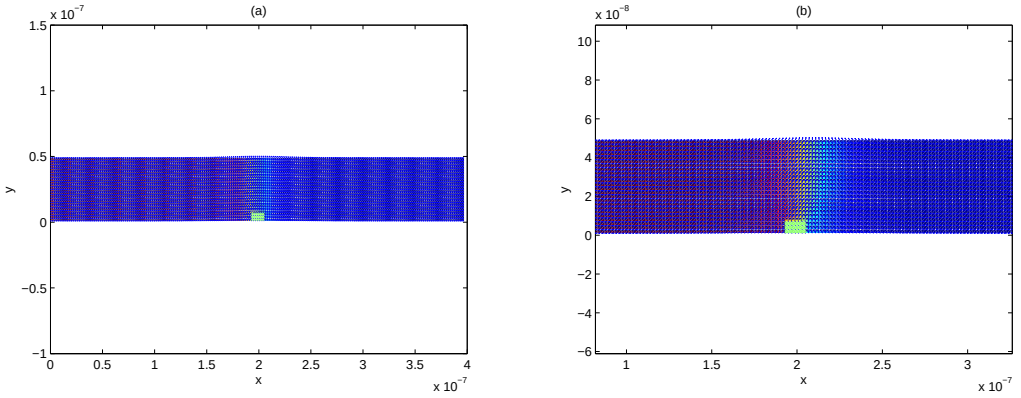


Figure 1: A geometrical construction formed by removing a rectangular defect at the edge of a magnetic nano strip with width 50 nm. (a) Initial stable transverse domain wall. The defect is at the center of the wall. (b) Domain structure under current $b_J = -700$ at $t = 0.015$ ns.

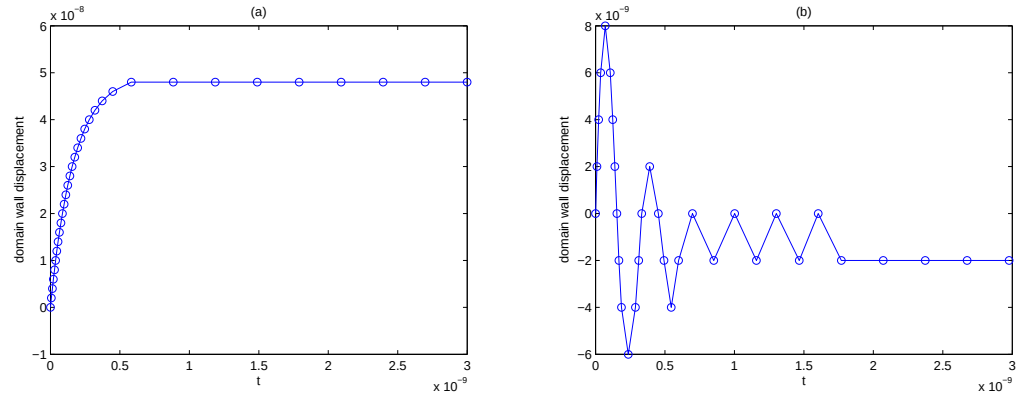


Figure 2: The domain wall displacement as a function of time under current $b_J = -300$ for a perfect nanostrip in (a), and a nanostrip with a 12×10 nm^2 defect on one edge in (b).

direction of the current. The stray field is taken as the shape anisotropy $4\pi M_s$ due to the thin strip model. The damping parameter α is fixed to be 0.02, and the material parameters are: the saturation magnetization $M_s = 14.46 \times 10^5$ A/m, the exchange constant $A = 2. \times 10^{-7}$ erg/cm, the anisotropy $H_K = 500$ Oe, $\gamma = 1.76 \times 10^7\ Oe^{-1}s^{-1}$.

The initial stable domain wall is at the center of the defect on one edge of the strip as shown in Fig. 1 (a). Under a current, the geometrically confined domain wall structure is shown in Fig. 1 (b). When a current is applied along the direction of the long axis of the strip, the domain wall begins to move opposite to the direction of the current. If the current is smaller than the critical values, the domain wall oscillates around the center of the defect. The oscillation amplitude decreases with time due to the Gilbert damping, and the wall eventually stops at the defect. The domain wall displacement as a function of time is shown in Fig. 2 (b), for the 12×10 nm^2 defect and the applied current $b_J = 300$ antiparallel to the long axis of the strip. For comparison, the displacement for the perfect

https://doi.org/10.4208/eajam.181016.300517d Published online by Cambridge University Press

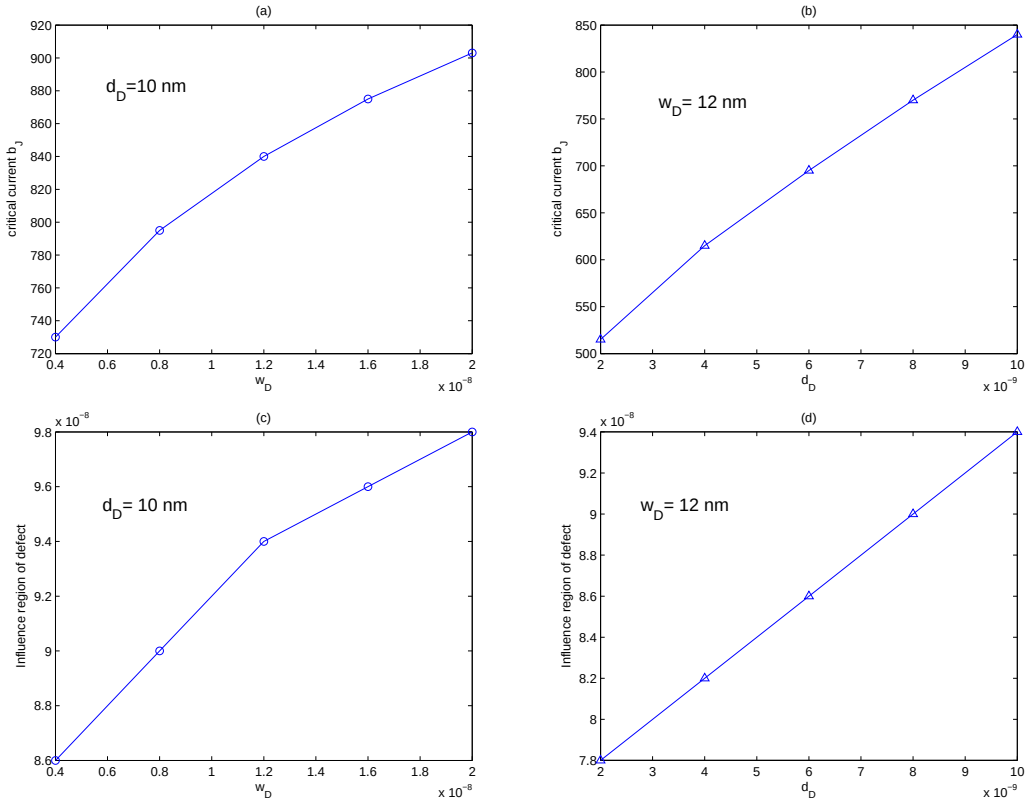


Figure 3: (a) The critical current for the depinning of the wall as a function of the width of the defect on one edge with fixed defect depth $d_D = 10$ nm. (b) The critical current for the depinning of the wall as a function of the height of the defect with fixed width $w_D = 12$ nm. The maximum displacement of the wall under the critical current for different defect as a function of the width or the height of the defect are shown in (c) and (d).

strip with the same current is shown in Fig. 2 (a). The effect of the defect on the domain wall motion is apparent. The maximal displacement is 48 nm without defect and only 8 nm for the strip with defect.

When the current is sufficiently large, the domain wall will be able to escape from pinning by the defect. We define the critical electric current as the minimum values required for the depinning of the wall. The critical values of the current depend on the size of the defects. We compare the critical current and the effect region for various height d_D and width w_D of the defects in Fig. 3. Fig. 3 (a) and (c) show the critical currents and their effecting region for different widths w_D with fixed depth $d_D = 10$ nm. For different depths d_D with fixed width $w_D = 12$ nm, the comparisons are shown in Fig. 3 (b) and (d). The values of the critical current and the effected region illustrate that the height of the defect has stronger effect on the wall dynamics. The pinning potential is stronger when the defect is higher. It is interesting to take a look at the domain wall mobility in the vicinity of the defect. To observe the domain wall propagation clearly, we consider two symmetrical defects with the same size at both edges of the strip. The size of the defect is $w_D = 16$

https://doi.org/10.4208/eajam.181016.300517d Published online by Cambridge University Press

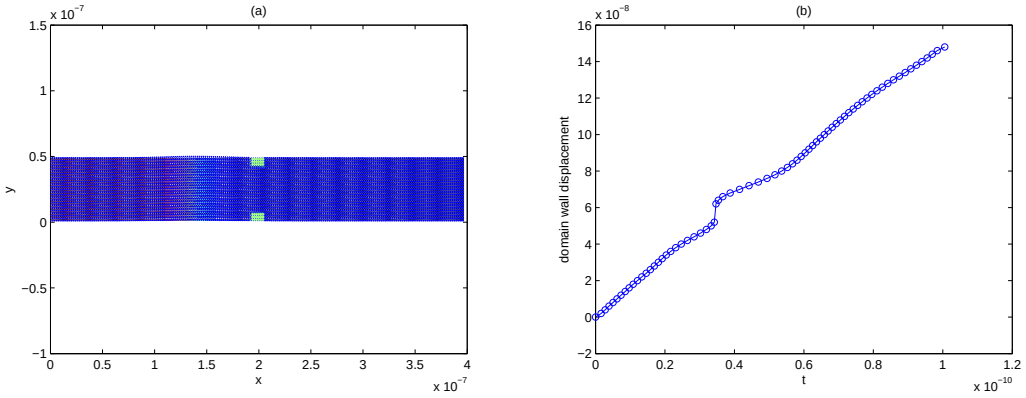


Figure 4: (a) Geometry of the strip with two symmetrical defects at both edges of the strip, and the initial transverse wall is away from the defects. (b) The displacement of the domain wall as a function of time under current $b_J = -1800$, and both defect size is 16×12 nm^2.

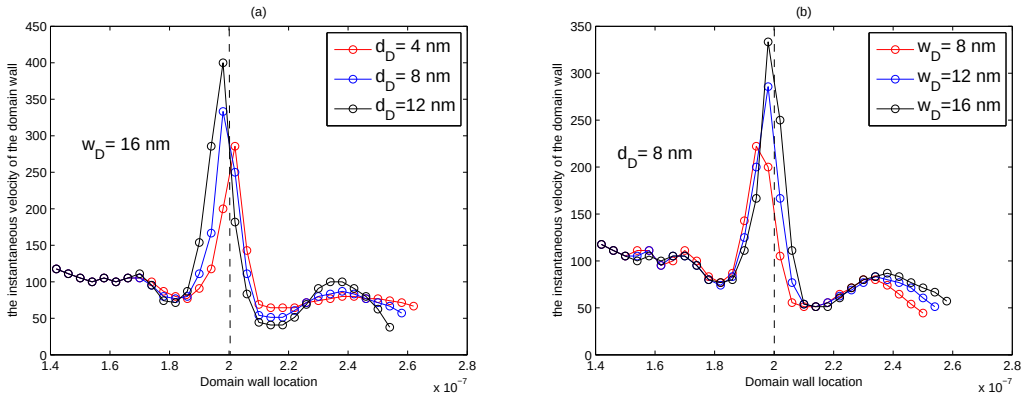


Figure 5: The instantaneous velocity of the domain wall versus its location for the defects with different size.

and $d_D = 12$. The initial domain wall position is 60 nm away from the defect position as shown in Fig. 4 (a). The applied current is $b_J = 1800$ which is large enough to overcome the pinning potential of the defect. The displacement of the wall is shown in Fig. 4 (b). When the domain wall arrives to the left side of the defect, it moves moves faster suddenly as dropping into the defect, and moves slowly inside the defect. When it goes out of the defect, the defect can accelerate the moving as pushing the wall away from it.

To illustrate the effect of the defect, in Fig. 5, we plot the velocity of the domain wall as a function of x and for various size of defects and the applied current is $b_J = -1600$. When the domain wall is sufficiently close to the defect, it experiences a strong attracting force from the defect and starts to accelerate until it reaches the maximum velocity at the defect center. The velocity then starts to decrease due to the same attracting force. The maximum velocity increases with the size of the defect.

In conclusion, when the domain wall passes through a defect, it experiences an attrac-

https://doi.org/10.4208/eajam.181016.300517d Published online by Cambridge University Press

tion force so that it accelerates before it reaches the center of the defect and it slows down after it passes the defect. This attraction force increases with the size of the defect. There is a critical current b_{Jc} above which the domain wall will be able to escape this attraction force due to the defect and continue to move along the wire. On the other hand, below the critical current, the domain wall oscillates around the defect and eventually stops. Our results also indicate that the critical current b_{Jc} is affected more by the height of the defect than the width of the defect. A pinning potential can be constructed to model the effect of defect which is explained in the next section.

4. Amplification of Domain Wall Motion

As is shown in Section 3, the injection of current below a threshold (critical value) through a domain wall confined to a pinning potential results in its processional motion within the potential well. From experimental results and numerical results in a simple 1D model, Luc. Thomas [16] shows that the motion of domain walls under nanosecond-long current pulses is surprisingly sensitive to the pulse length. By using a short train of current pulses, whose length and spacing are tuned to the precession frequency, the domain wall's oscillations can be resonantly amplified, which makes it possible to reduce the critical current for driving the domain wall motion. The study of the domain wall dynamics driven by AC current is a new consideration and is investigated in this paper.

In this section, we study the domain wall motion in a nanowire along x axis in a one dimensional model with an artificial pinning potential to model the defect. The domain wall motion is studied under different kind of current: DC current, nanosecond-long current pulses and AC current flows. We focus on the amplification of the wall oscillation induced by AC current compared with that driven by DC current, which is studied for the first time mathematically.

The generalized dynamic equation of the magnetization is described by Landau-Lifshitz equation with the spin transfer torque as in Eq. (2.4). In general, a pinning effect exists in the micromagnetic experiments created by a defect in the nano particle as we have shown in Section 3. In our one dimensional calculation, a simplified pinning potential H_p [16,17] is adopted with the strength of the pinning potential K_p depending on the size of defect, and the width of the pinning potential q_0. The pinning potential is usually written in the form:

$$H_p = \begin{cases} 0 & |d-d_0| >= q_0, \\ \pm 2K_p \dfrac{d-d_0}{q_0} & |d-d_0| < q_0. \end{cases} \tag{4.1}$$

where d is the position of the domain wall center, d_0 is the defect position. The sign before K_p is positive for the tail-to-tail wall and negative for the head-to-head wall. In our calculations, we focus on the tail-to-tail wall.

https://doi.org/10.4208/eajam.181016.300517d Published online by Cambridge University Press

The effective field $\mathscr{H}_{eff}$ is written explicitly as:

$$\begin{aligned}\mathscr{H}_{eff} =&\gamma\left(\frac{H_K M_1}{M_s}e_x + \frac{2A}{M_s^2}\triangle\mathbf{M} - 4\pi M_3 e_z + H_e e_x + H_p e_x\right)\\ &+ \frac{b_J}{M_s^2}\mathbf{M}\times\frac{\partial\mathbf{M}}{\partial x} + \frac{c_J}{M_s}\frac{\partial\mathbf{M}}{\partial x},\end{aligned} \tag{4.2}$$

where H_K is the anisotropy constant, A is the exchange coefficient, and $4\pi M_3$ is the simplified demagnetization field as the shape anisotropy.

To solve the magnetization vector as a function of position x and time t, we use the fourth-order Runge-Kutta method. Initially, the domain wall at $d_0 = 0$ is a Neel wall in the following form $\theta = \pi - 2\tan^{-1}\exp(x/W_0)$, $\varphi = 0$, where $W_0 = \sqrt{2A/H_k M_s}$ is the initial domain wall width. In the following numerical calculations, we consider the parameters: $M_s = 8\times10^5$ A/m, $A = 1.3\times10^{-11}$J/m, $H_K = 500$ Oe, $\gamma = 1.76\times10^7$Oe^{-1}s^{-1}, $q_0 = 50$ nm and the damping parameter $\alpha = 0.008$.

In polar coordinates, the magnetization vector $\mathbf{M}$ can be described by θ which represents the angle between the magnetization vector and the x axis, and φ which is the out of plane angle of the magnetization vector projected in the yz plane. We focus on the domain wall dynamics described by the domain wall displacement and the out of plane component m_3.

4.1. Domain wall motion induced by DC current with pinning effect

The effect of pinning potential on the dynamics of the domain wall motion is studied in this section. The initial domain wall is at the position of the pinning.

As is shown in Section 3, for a perfect nanostrip without defect, when a current is applied along the x axis, the domain wall moves away from the initial position opposite to the current direction and the magnetization of the domain wall is no longer confined in the wide plane of the nanostrip. The velocity of the domain wall decreases and eventually the domain wall stops with a fixed nonzero m_3 component. The maximal displacement of domain wall depends on the amplitude of the current. There is a critical current, above which the domain wall will be distorted.

In the first example, we set the strength of the pinning potential $K_P = 20000$ and $\xi = 0$ and apply a current with $b_J = -50$. Initially, the domain wall is located at the center of the defect. The dynamics of the domain wall is similar to that presented in Section 3. When the current is applied, the domain wall starts to move. Since the current is not strong enough, it oscillates around the defect and eventually stops at the defect center. In Fig. 6, the domain wall position and maximum of m_3 are plotted as a function of time. As we increase the current density b_J, the maximum displacement increases as is shown in Fig. 7. Maximum value of out of plane component m_3 has the similar behavior.

We compare the maximal displacement of the domain wall by applying different current with fixed pinning potential $K_p = 20000$ and $\xi = 0$. The maximal displacement and maximum m_3 are functions of increasing current as shown in Fig. 7. It is necessary to apply

https://doi.org/10.4208/eajam.181016.300517d Published online by Cambridge University Press

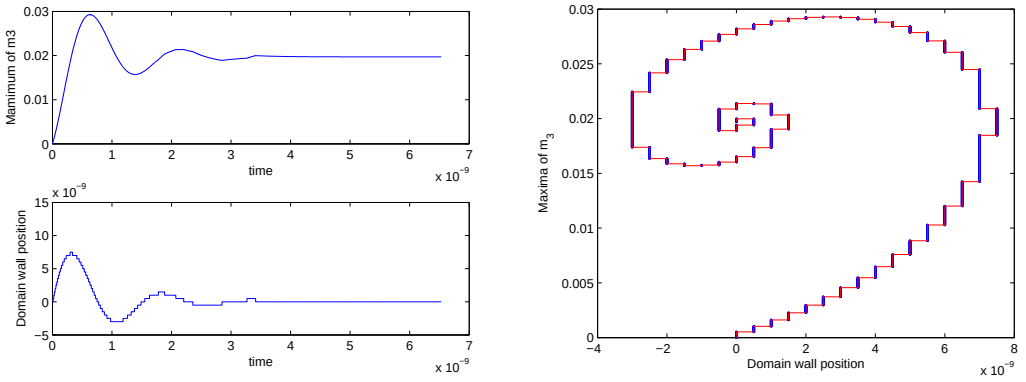


Figure 6: The out of plane component m_3 of the domain wall and position of the domain wall as functions of time in (a). Trajectory of the domain wall in the phase space (p, m_3)(p the domain wall displacement) in (b). Current $b_J = -50$, $K_p = 20000$.

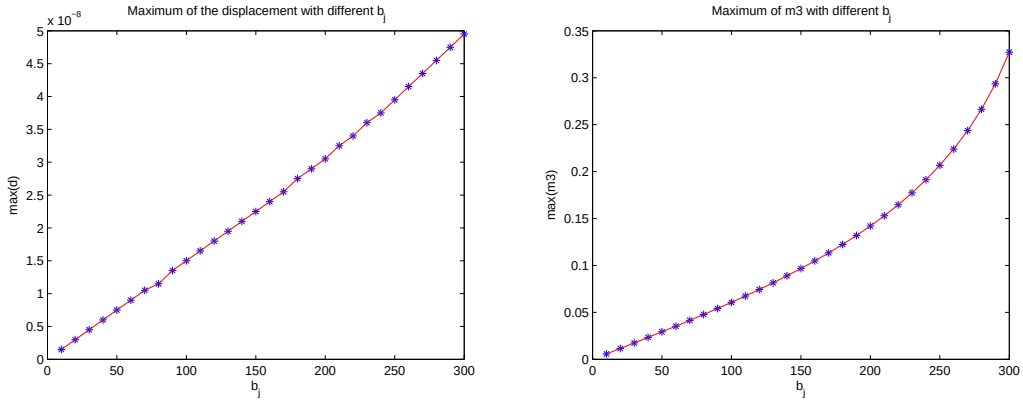


Figure 7: The maximum domain wall displacement and maximum m_3 at the wall center as functions of current. K_p=20000. $\xi = 0$.

stronger current to move the domain wall in larger oscillation as the domain wall pinned by the defect.

The critical current is defined as the minimum value required for the depinning of the domain wall. If the current is stronger than the critical value, the domain wall will be able to escape from the pinning and eventually move away from the defect. This critical current depends on the strength and width of the pinning potential. In Fig. 8 (a), we show the domain wall displacement for different b_J but with a fixed pinning potential. It is obvious that given a defect, there is an intrinsic oscillation potential that is independent of the current. On the other hand, the oscillation frequency increases with the strength of the pinning potential as shown in Fig. 8(b).

Actually, the role of the nonadiabatic torque is very similar to the magnetic field [6]. The domain wall oscillates around a new equilibrium position under a DC current. Fig. 9 shows the maximal displacement and the new equilibrium position as functions of ξ which

https://doi.org/10.4208/eajam.181016.300517d Published online by Cambridge University Press

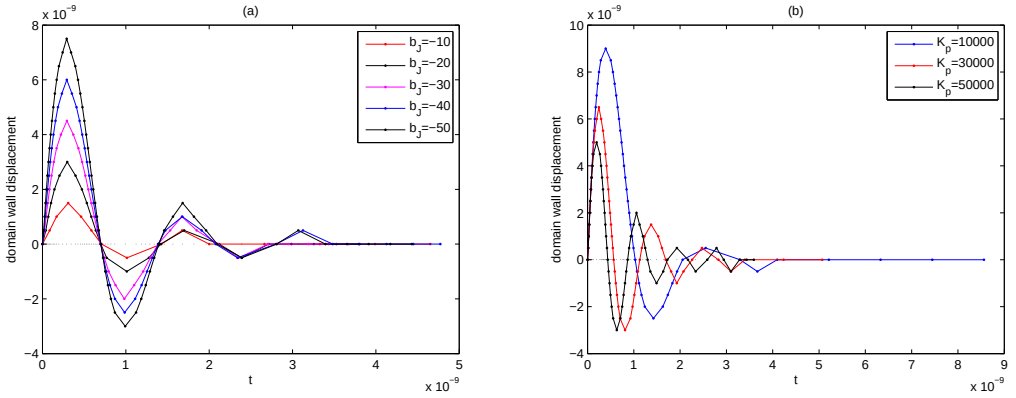


Figure 8: (a) The displacement of the domain wall oscillation under different DC current b_J with fixed $K_p = 20000$. (b) The displacement of the domain wall oscillation for different K_p under DC current $b_j = -50$. $\xi = 0$.

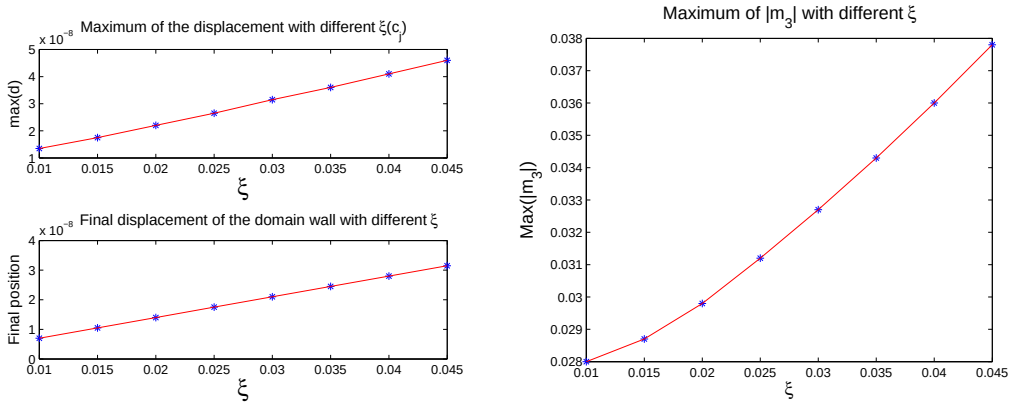


Figure 9: The maximum displacement and final position of the domain wall as functions of ξ with fixed $K_p = 20000$ and current $b_J = -50$. The magnetization component m_3 as a function of ξ.

is linear in the left figure, and the maximal m_3 increases with increasing ξ as shown in the right figure. In the calculations, we also find that the frequency of the domain wall position oscillation is lower for larger ξ.

4.2. Amplification of magnetic domain wall motion by pulses and AC current

In reality, the critical current for driving the domain wall is too high for application purpose. One way to reduce the threshold value was presented by Luc. Thomas [16] that the oscillations in the domain wall position can be resonantly amplified by using a short sequence of current pulses, whose lengths and separations are tuned to its oscillation frequency.

In our calculation, we show the domain wall position and maximal m_3 (Fig. 10) as functions of time under two current pulses of same amplitude with different pulse precession

https://doi.org/10.4208/eajam.181016.300517d Published online by Cambridge University Press

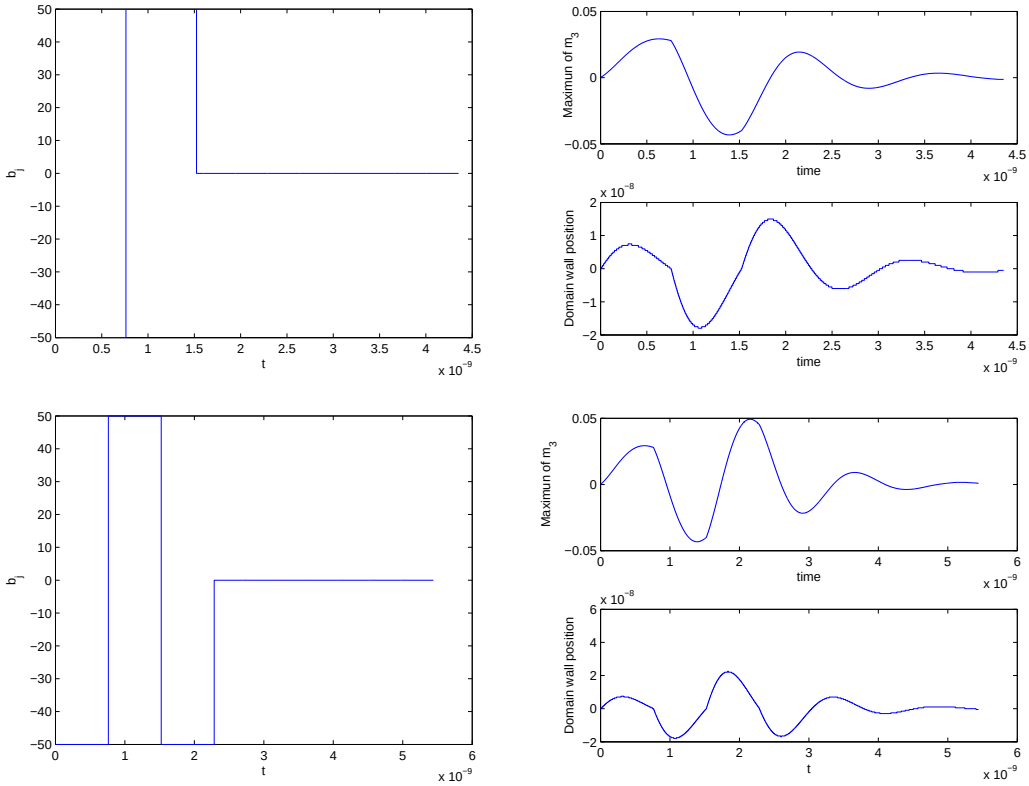


Figure 10: Two pulses of the same amplitude with different periods vs the corresponding domain wall displacement, and magnetization component m_3 as functions of time. $K_p = 20000$, $\xi = 0$.

periods, for fixed $K_p = 20000$ and $\xi = 0$.

The current pulses with different precession periods lead to different domain wall motion. When DC current is applied, the domain wall oscillation has an intrinsic frequency which depends only on the defect. It is then possible to amplify this domain wall oscillation from the resonance effect by applying a pulse current with appropriate frequency. We compare the maximal displacement and m_3 for current pulses with different frequencies for fixed pinning potential in Fig. 11. The amplification of domain wall position is the strongest when the period of current pulse is 1.4ns with parameters $K_p = 20000$, $\xi = 0$.

It is obvious that AC current with a suitable frequency can amplify the domain wall position oscillation more than the pulse current with the same amplitude. Here, we consider an AC current $bj = -50\cos(2\pi t/T)$. The current amplitude is 50 and T is the current period $1/f$ (f is the frequency). The AC current is unsteady, thus the nonadiabatic spin torque has to be involved in the calculation. The typical value of ξ who describes c_j/b_j is within the range of 0.0025-0.04 [18]. We use the value $\xi = 0.01$ and the strength of pinning potential $K_p = 20000$. Fig. 12 shows the current with $T = 1.0$ ns, the corresponding maximum value of m_3 and the domain wall displacement as functions of time. The trajectory of the domain wall in the phase space (p, m_3) is shown in Fig. 13.

https://doi.org/10.4208/eajam.181016.300517d Published online by Cambridge University Press

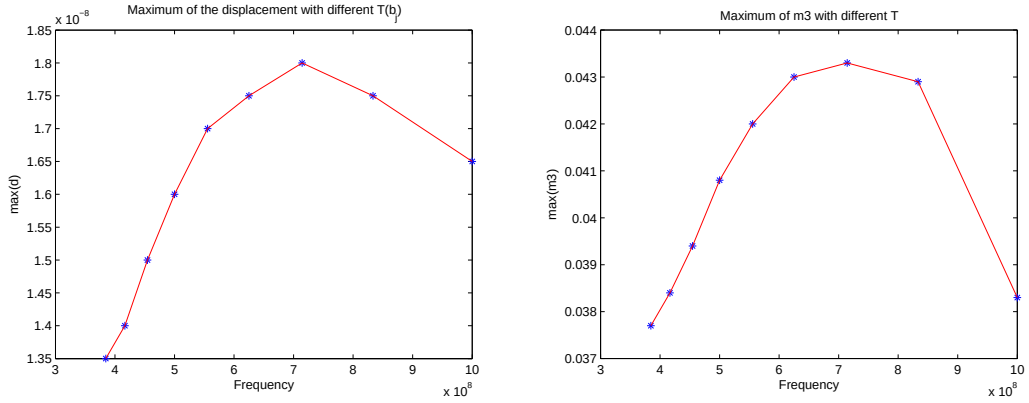


Figure 11: The maximum values of the domain wall displacement and m_3 at the domain wall center under current pulses with different frequencies. $K_p = 20000$, $\xi = 0$.

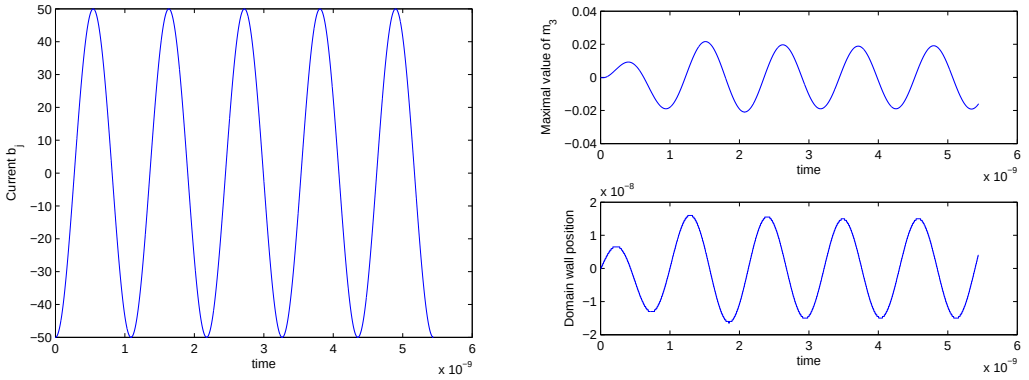


Figure 12: With AC current $b_J = -50\cos(2\pi t/T)$ whose amplitude is 50 and period $T = 1.0$ ns, the corresponding domain wall displacement and magnetization component m_3 as functions of time. Trajectory of domain wall in the phase space (p, m_3).

The maximal values of the domain wall displacement and m_3 in the oscillations depend on the amplitude and the frequency of the ac current. The domain wall will oscillate with the same frequency as that of the AC current. We show in Fig. 14 the maximum displacement (oscillation amplitude) and the maximum value of m_3 as a function of the frequency of the AC current. It is clear that the oscillation amplitude attains maximum with a frequency which is close to the intrinsic frequency of the potential with strength $K_p = 20000$ under DC current. The oscillation amplitude as a function of the frequency of the ac current behaves like a Gaussian distribution.

5. Conclusion

In conclusion, when the domain wall passes through a defect, it experiences an attraction force so that it accelerates before it reaches the center of the defect and it slows down

https://doi.org/10.4208/eajam.181016.300517d Published online by Cambridge University Press

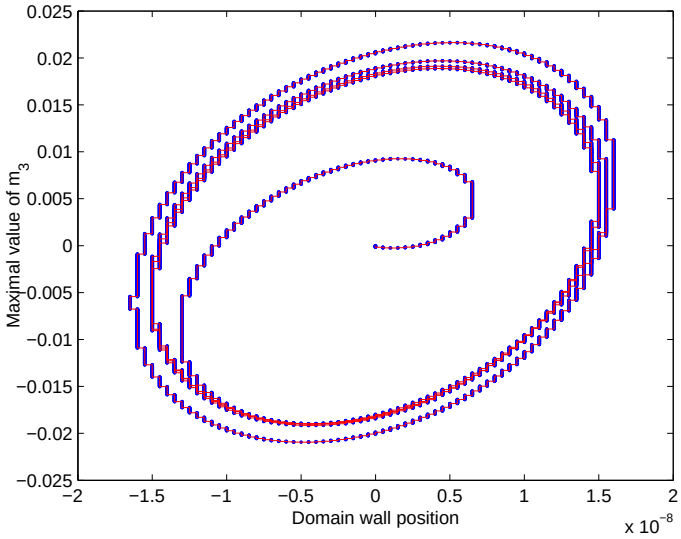


Figure 13: Trajectory of domain wall in the phase space (p, m_3) with AC current $b_J = -50\cos(2\pi t/T)$.

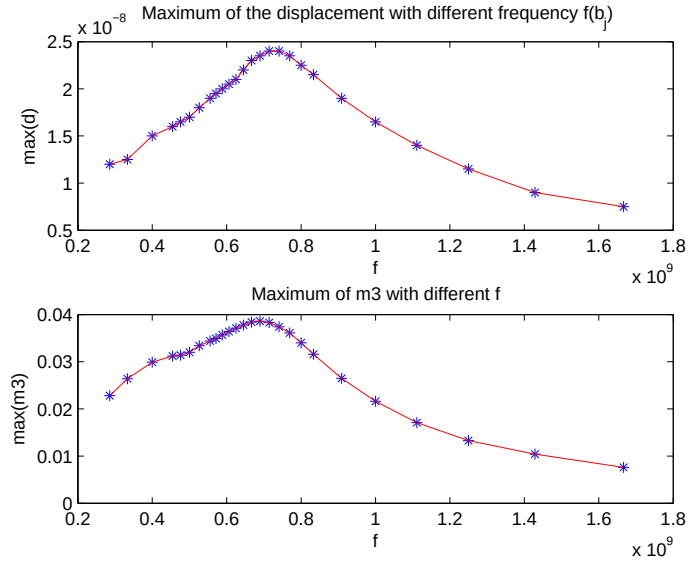


Figure 14: The maximum domain wall displacement and maximum value of m_3 at the domain wall center as functions of the frequency of the AC current. $K_p = 20000$, $\xi = 0.01$.

after it passes the defect. On the other hand, below the critical current, the transverse domain wall oscillates damply and finally stops at the defect site in nanostrip. The critical current for the transverse wall depinning depends on the size of the rectangular defect and is affected more by the height of the defect. For a fixed defect, there is an intrinsic oscillation potential which is independent of the strength of the applied current. The am-

https://doi.org/10.4208/eajam.181016.300517d Published online by Cambridge University Press

plification of the transverse wall oscillation for both displacement and maximum value of m_3 is significant by applying AC current and current pulses with appropriate frequency in our numerical study. The oscillation amplitude as a function of the frequency of the AC current behaves like a Gaussian distribution. This investigation would be useful to design optimal parameters to control and manipulate domain wall motion in magnetic recording devices.

Acknowledgments

I would like to thank professor X.P. Wang for helpful discussions and support. This work was supported by FDCT 101/2016/A3, and National Natural Science Foundation of China (11701598).

References

[1] J. Chen, L. Yang and X.P. Wang, *The sharp interface limit of domain wall dynamics in Landau-Lifshitz equation and Walker's ansatz*, Commun. Math. Sci., Under review.
[2] Y. Chen, F. Huang, *Spectral method approximation of flow optimal control problems with H^1-norm state contraint*, Numer. Math.-Theory Methods Appl. **10**, 614-638 (2017)
[3] W.N. E and X.P. Wang, *Numerical methods for the Landau-Lifshitz equation*, SIAM J. Numer. Anal. **38**, 1647-1665 (2001).
[4] N.L. Gibson, *A Polynomial Chaos Method for Dispersive Electromagnetics*, Commun. Comput. Phys. **18**, 1234-1263 (2015).
[5] J. Grollier, V. Cros, A. Hamzic, J.M. George, H. Jaffres, A. Fert, G. Faini, J. Ben Youssef and H. Legall, *Spin-polarized current induced switching in Co/Cu/Co pillars*, Appl. Phys. Lett. **78**, 3663 (2001).
[6] J. He, Z. Li and S. Zhang, *Current-driven domain-wall depinning*, J. Appl. Phys. **98**, 016108 (2005).
[7] D. Ilgaz, J. Nievendick, L. Heyne, D. Backes, J. Rhensius, T.A. Moore, M.á. Niño, A. Locatelli, T.O. Menteş, A.v. Schmidsfeld, A.v. Bieren, S. Krzyk, L.J. Heyderman and M. Kläui, *Domain-wall depinning assisted by pure spin currents*, Phys. Rev. Lett. **105**, 076601 (2010).
[8] J.A. Katine, F.J. Albert, R.A. Buhrman, E.B. Myers and D.C. Ralph, *Current-driven magnetization reversal and spin-wave excitations in Co /Cu /Co pillars*, Phys. Rev. Lett. **84**, 3149 (2000).
[9] S.D. Kim, B.S. Chun and Y.K. Kim, *Domain wall width and velocity behaviors in notched magnetic devices*, J. Appl. Phys. **101**, 09F504 (2007).
[10] Z. Li and S. Zhang, *Domain-wall dynamics driven by adiabatic spin-transfer torques*, Phys. Rev. B **70**, 024417 (2004).
[11] T. Ono, H. Miyajima, K. Shigeto and T. Shinjo, *Magnetization reversal in submicron magnetic wire studied by using giant magnetoresistance effect*, Appl. Phys. Lett. **72**, 1116 (1998).
[12] M. Poluektov, O. Eriksson, G. Kreiss, *Scale transitions in magnetisation dynamics*, Commun. Comput. Phys. **20**, 969-988 (2016).
[13] S. Parkin, M. Hayashi and L. Thomas, *Magnetic domain-wall racetrack memory*, Science **320**, 190-194 (2008).
[14] S. Parkin and S.H. Yang, *Memory on the racetrack*, Nature Nanotechnol. **10**, 195-198 (2015).
[15] J.Z. Sun, *Current-driven magnetic switching in manganite trilayer junctions*, J. Magn. Magn. Mater. **202**, 157-162 (1999).

https://doi.org/10.4208/eajam.181016.300517d Published online by Cambridge University Press

[16] L. Thomas, M. Hayashi, X. Jiang, R. Moriya, C. Rettner and S. Parkin, *Oscillatory dependence of current-driven magnetic domain wall motion on current pulse length*, Nature **443**, 197 (2006).
[17] L. Thomas, M. Hayashi, X. Jiang, R. Moriya, C. Rettner and S. Parkin, *Resonant amplification of magnetic domain-wall motion by a train of current pulses*, Science Reports, **315**, 1553 (2007).
[18] A. Thiaville, Y. Nakatani, J. Miltat and Y. Suzuki, *Micromagnetic understanding of current-driven domain wall motion in patterned nanowires*, Europhys. Lett. **69**, 990-996 (2005).
[19] L. Thomas, C. Rettner, M. Hayashi, M.G. Samant, S.S.P. Parkin, A. Doran and A. Scholl, *Observation of injection and pinning of domain walls in magnetic nanowires using photoemission electron microscopy*, Appl. Phys. Lett. **87**, 262501 (2005).
[20] X.P. Wang, C.J. Garcia-Cervera and W.N. E, *A Gauss-Seidel projection method for micromagnetics simulations*, J. Comput. Phys. **171**, 357-372 (2001).
[21] J.E. Wegrowe, D. Kelly, T. Truong, Ph. Guittienne and J.Ph. Ansermet, *Magnetization reversal triggered by spin-polarized current in magnetic nanowires*, Europhys. Lett. **56**, 748-754 (2001).
[22] X. Han, Y. Li and H. Xie, *A multilevel correction method for Steklov eigenvalue problem by nonconforming finite element methods*, Numer. Math.-Theory Methods Appl. **8**, 383-405 (2015).
[23] L. Yang, *Current Induced Domain Wall Motion: Analysis and Simulation*, Ph.D Thesis, 2008.
[24] H.Y. Yuan and X.R. Wang, *Domain wall pinning in notched nanowires*, Phys. Rev. B **89**, 054423 (2014).
[25] L. Yang and X.P. Wang, *Dynamics of domain wall in thin film driven by spin current*, Discrete Contin. Dynam. Syst. Ser. B **14**, 1251-1263 (2010).
[26] S. Zhang, P.M. Levy and A. Fert, *Mechanisms of spin-polarized current-driven magnetization switching*, Phys. Rev. Lett. **88**, 236601 (2002).
[27] S. Zhang and Z. Li, *Roles of nonequilibrium conduction electrons on the magnetization dynamics of ferromagnets*, Phys. Rev. Lett. **93**, 127204 (2004).

https://doi.org/10.4208/eajam.181016.300517d Published online by Cambridge University Press